Tunnelling and Underground Space Technology 107 (2021) 103655

Contents lists available at ScienceDirect

Tunnelling and Underground Space Technology incorporating Trenchless Technology Research

journal homepage: www.elsevier.com/locate/tust

Development of a real-time muck analysis system for assistant intelligence TBM tunnelling

Qiuming Gong [a,*], Xiaoxiong Zhou [a], Yongqiang Liu [b], Bei Han [a], Lijun Yin [a]

[a] Key Laboratory of Urban Security and Disaster Engineering of Ministry of Education, Beijing University of Technology, Beijing 100124, China
[b] Beijing Jiurui Technology Co., Ltd, Beijing 100124, China

ARTICLE INFO

Keywords:
Tunnel boring machine
Assistant intelligence tunnelling
Machine vision
Deep learning
System design

ABSTRACT

Intelligent tunnelling has become an important direction for the development of TBM technology recently. As a result of the interaction between rock mass and TBM cutterhead, mucks are very important for predicting rock mass conditions and evaluating rock breaking efficiency. A real-time muck analysis system for assistant intelligence TBM tunnelling is proposed in this paper. Machine vision was applied to take the muck images continuously in the high-speed conveyor belt. The image segmentation and feature extraction of the mucks are conducted by using a deep learning algorithm. The proposed system also measured the mass and volume flow of the muck by installing a belt scale and a scanner to monitor the stability of the rock mass on the tunnel face. After the system was completed, it was installed on an indoor simulation experimental platform. A series of experiments were conducted to verify the design functions and measurement accuracy. Additionally, the system was applied to a TBM tunnelling project. The application results showed that the proposed system reached its design requirements and functions, and can provide muck data support for further assistant intelligent TBM tunnelling.

1. Introduction

With the development of the manufacturing industry and construction technology, more deep and long tunnels use TBMs construction due to their advantages of low cost and high tunnelling efficiency. However, complicated geological conditions bring great challenges to TBM construction. More specifically, on the one hand, because the rock mass conditions ahead of the tunnel face are not clear, so this increases the risks of TBM construction, such as jamming, rockburst, or even tunnel collapse. On the other hand, the selection of operating parameters is dependent on the experience of construction operators, which may cause problems such as low TBM tunnelling efficiency, abnormal consumption of cutting tools, and machine failures. To solve these two fundamental problems, namely the prediction of rock mass conditions and the evaluation of tunnelling efficiency, researchers have conducted extensive studies in these areas recently.

In most studies, the prediction of TBM tunnelling performance, which is required for progress schedule and cost control, has always been a research hotspot. Based on TBM boring parameters (e.g., thrust and torque) and rock mass parameters (e.g., rock strength and volumetric joint count), many researchers (Barton, 2000; Bruland, 2000; Gong and Zhao, 2009; Hamidi et al., 2010; Liu et al., 2017; Maleki, 2018; Naghadehi et al., 2018; Rostami, 1997; Salimi et al., 2018; Vergara and Saroglou, 2017) have established various models to predict tunnelling performance. These types of studies are forward analysis methods and are generally used for cost estimation in the early stage of the project. However, the rock mass parameters in the actual construction cannot be accurately obtained, so these models are difficult to guide the tunnelling in real-time.

In the past ten years, some researchers tried to solve these problems by monitoring and analyzing the data in TBM tunnelling. The monitoring technologies for TBM are mainly about the forces of disc cutters (Entacher and Galler, 2013; Entacher et al., 2012) and the interaction between the TBM and the surrounding rock mass (Huang et al., 2018). Although there is a specific correlation between these monitoring data and the rock mass conditions (Entacher et al., 2013), this relationship is poorly interpretable and needs to be further explored by mining the monitoring data. The photographic documentation of the tunnel face (Entacher and Galler, 2013) and ahead geology forecast (Li et al., 2017, 2018) directly investigate the geological conditions in front of the tunnel face. Nevertheless, these technologies are difficult to wholly and continuously monitor the entire tunnelling process. Apart from this,

* Corresponding author.
E-mail address: gongqiuming@bjut.edu.cn (Q. Gong).

https://doi.org/10.1016/j.tust.2020.103655
Received 18 March 2020; Received in revised form 11 September 2020; Accepted 28 September 2020
Available online 21 October 2020
0886-7798/© 2020 Elsevier Ltd. All rights reserved.

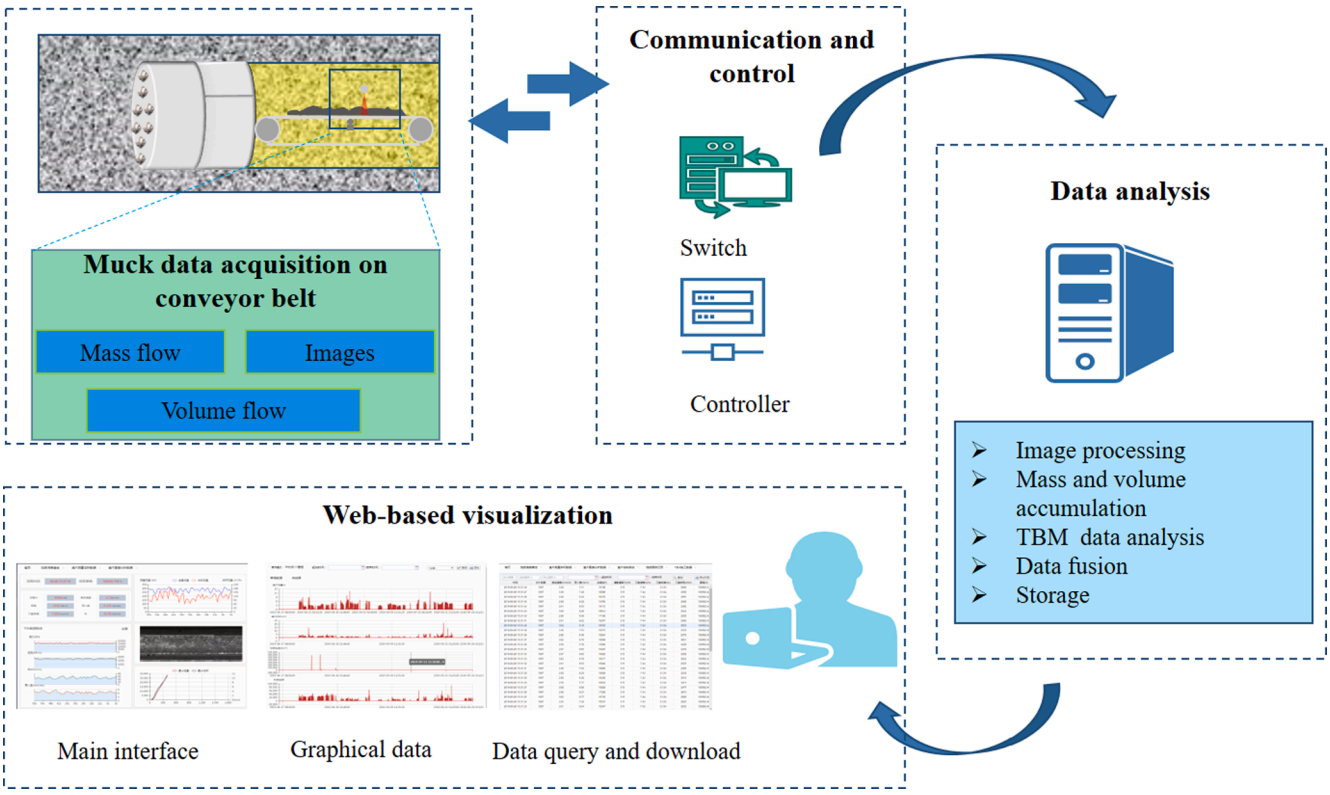

Fig. 1. The framework of the muck analysis system.

different degrees of personnel participation is required for sensors installation and data analysis and increases the operating cost of these technologies. In fact, many sensors equipped on the TBM are used to monitor the operating parameters of different parts of the device in real-time (Gao et al., 2019; Sun et al., 2018; Zhang et al., 2019; Zhao et al., 2019). There are a few parameters related to the interaction between the surrounding rock mass and TBM. Among these related parameters, most control parameters are inputted by human beings, while few parameters are fed back by the rock mass. Therefore, the information contained in the TBM data that can be used to evaluate the rock mass is limited.

During the TBM tunnelling progress, the disc cutters cut the rock mass to form rock chips. The features of muck are determined by the boring parameters and rock mass properties. It is a back-analysis method to evaluate the TBM tunnelling efficiency and identify the rock mass parameters by analyzing the characteristics of chips. A large number of researchers explored the relationship between the characteristics of rock chips and rock-breaking efficiency, and found that they are closely connected to each other. Specifically, when using the specific energy (SE) to evaluate the rock-breaking effectiveness, the roughness index (CI), calculated from the size distribution of the rock chips, is inversely related to the SE (Abu Bakar et al., 2014; Mohammadi et al., 2020; Tuncdemir et al., 2008). This result shows that the higher the rock-breaking efficiency, the larger the size of rock chips. Besides, in the intact rock mass, when the rock-breaking efficiency is high, the shape of the large rock chips will be closer to flat (Bruland, 2000; Gong et al., 2007; Heydari et al., 2019). Based on the excellent correlation between rock chips characteristics and rock breaking effectiveness, some researchers use the rock chip characteristics to evaluate the rock-breaking efficiency of the geometry of the cutting tools or the cutting geometric parameters, e.g., the type of disc cutter (Tuncdemir et al., 2008), the cutter's spacing (Liu et al., 2016), and the cutting depth ratio (Yin et al., 2014). Generally speaking, these studies are carried out under constant rock mass parameters. However, the rock mass conditions in the TBM construction are always changing. Therefore the influence of the rock mass parameters on the rock chip characteristics cannot be ignored.

To the best of our knowledge, few pieces of research have been done to explore the relationship between the rock chip characteristics and rock mass parameters until now. The joint conditions are the main parameters of the rock mass that affects the morphological characteristics of the rock chips. Although Rispoli et al. (2017) did not obtain a significant correlation between CI and rock mass rating (RMR) and geological strength index (GSI) through TBM field research, some results of numerical simulation show that the joint conditions, e.g., joint spacing and angle, affect the rock chip formation process (Gong et al., 2006, 2005; Jiang et al., 2018; Liu et al., 2019; Zhai et al., 2016). Yin et al. (2016) conducted full-scale cutting experiments on granite and found that two different failure modes can be obtained for the joint spacing of 100 mm and 400 mm, respectively. These two failure modes will generate different sizes and shapes of rock chips. Gong et al. (2010) studied the rock chip characteristics excavated in marble with three different layer thicknesses (namely thin, medium-thick and thick), and found that the rock chips excavated in the thin layer marble were larger and the tunnel face was more likely to be unstable.

From the results of in-site, laboratory, and numerical studies, we can conclude that the muck contains a wealth of information, which can be used to predict the rock mass conditions and evaluate rock-breaking efficiency. Some methods of muck analysis applied to TBM construction focus on the reuse of excavated material. Oggeri (2017) has established a classification for the availability of muck under different formation conditions and construction methods. In order to sort the material of the TBM in real-time, Erben (2016) developed a muck analysis system installed on the TBM, involving the mass flow monitoring, grain grading distribution analysis and chemical composition analysis. These works provide essential information for assisting intelligent tunnelling by muck analysis, such as techniques about mass flow monitoring and grain grading analysis. The grading distribution plays a vital role in muck analysis. However,.the size distribution of the rock chips is mainly obtained with the sieving method, and even the axial

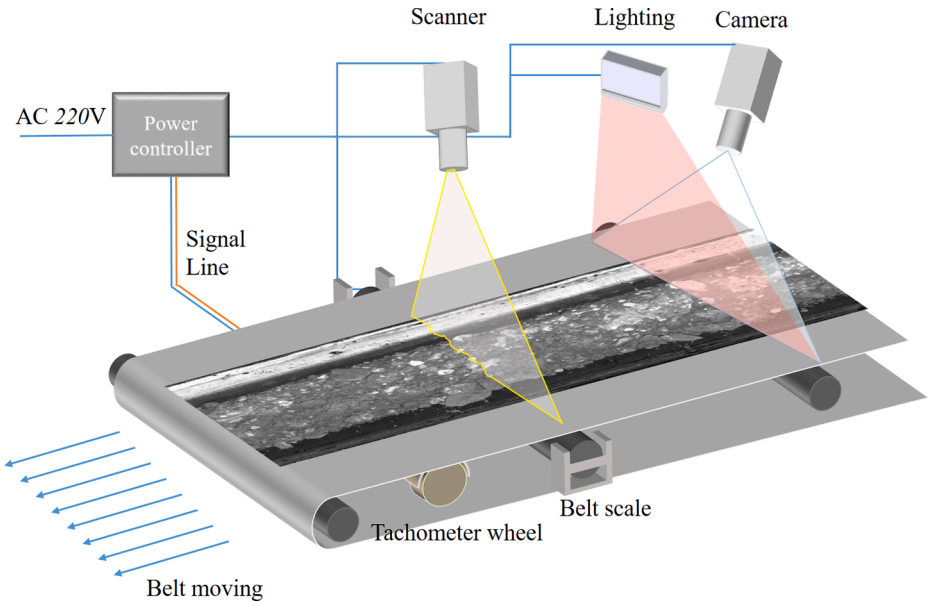

Fig. 2. The structure of the data acquisition system.

length of chips can only be measured manually. To collect statistically significant data, a high volume of mucks is required to be measured, which will be time-consuming and labour-intensive. Additionally, the data obtained by manual sieving is relatively lagging. Therefore, it is difficult to guide the real-time TBM construction. To improve the efficiency of muck analysis, Rispoli et al. (2017) evaluated the size distribution of muck by analyzing the images of muck in the muck yard and studied the relationships between the CI and the TBM performance parameters, as well as the rock mass parameters. Farrokh and Rostami (2008) also analysed the muck on the truck by using the image processing method, and studied the relationship between the size of rock chips and the tunnel convergence. This method can quickly obtain the grain grading distribution through image analysis software. Still, it is limited in that it is an off-line analysis method and cannot feedback information in real-time to the TBM operators. During the transportation of the muck from TBM to the muck yard, the rock chips have been transferred many times. As a result, the distribution of rock chips on the surface is changed. Bruland (2000) thinks that the most representative muck should be obtained directly from the conveyor belt. However, since the rock chips sampling from the conveyor belt requires stopping the belt, this will affect the TBM tunnelling (Rispoli et al., 2017). The machine vision approach can obtain fast and accurate results without contacting the objects, and is very suitable for the on-line analysis of muck on the TBM belt. However, the related researches in the present are scant.

Furthermore, the volume and mass of the muck are of great significance for monitoring the over-break of the TBM tunnels (Mooney et al., 2012; Slinchenko, 2009). By comparing the monitored and theoretical values of muck mass and volume, believe that the ground settlement caused by over-break in the TBM tunnel can be reflected (Mooney et al., 2012). In hard rock tunnels, over-break is mainly due to TBM encountering fractured zones or unstable rock masses (Barton, 2000). Therefore, monitoring the mass and volume of the muck is helpful to prevent instability of the tunnel face and to avoid further risk of jamming.

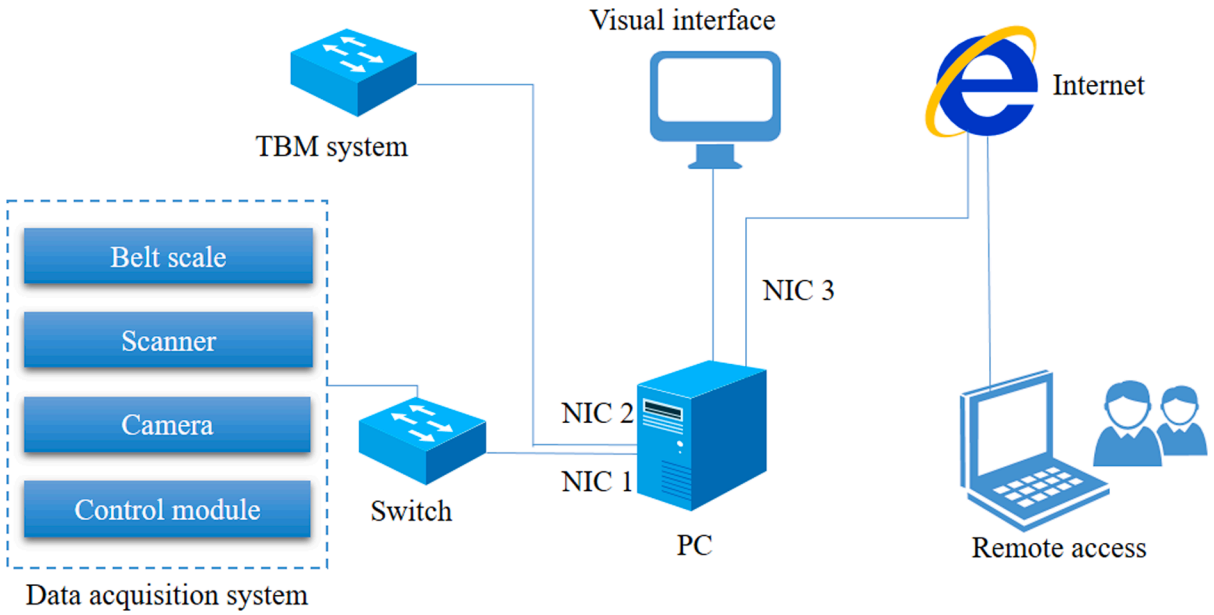

Fig. 3. The structure of the data acquisition system.

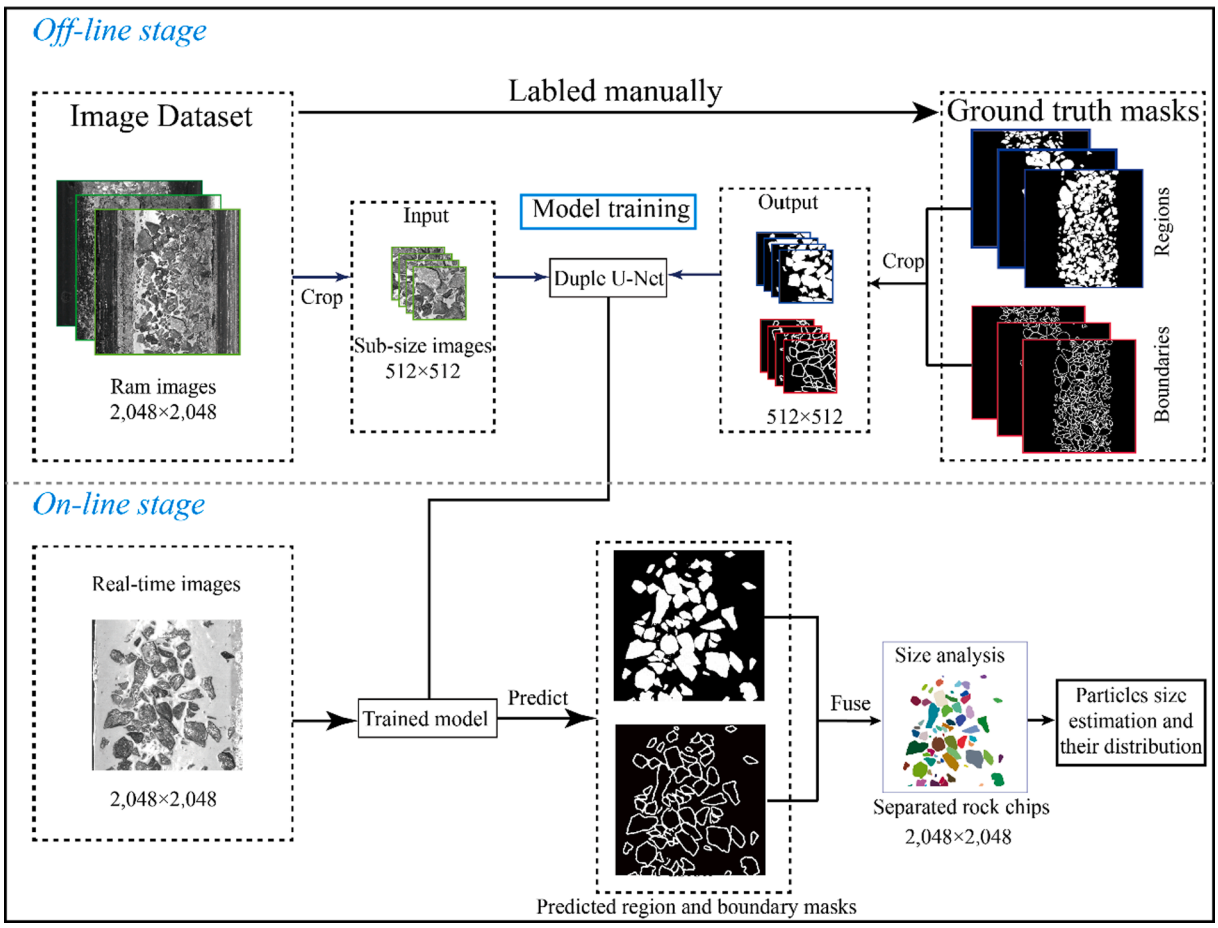

Fig. 4. Flow chart of chip segmentation and feature extraction.

To solve the abovementioned problems, this paper proposes a machine vision based system for on-line muck analysis in TBM tunnelling. This system directly collects images, mass flow and volume flow of muck on TBM conveyor belt, and performs image processing algorithms to extract the rock chip characteristics. Since it is a non-contact monitoring method, it can be synchronized with the TBM tunnelling. The analysis results can be fed back to the operator in real-time, thereby assisting in optimizing TBM operating parameters and judging rock mass parameters, and providing early warning of the instability of the tunnel face. This paper will introduce the design and composition of the system, image analysis methods, and the preliminary application results.

2. System composition

The system consists of four parts: data acquisition subsystem, communication and control subsystem, data analysis subsystem, and software subsystem. The structure of the system is illustrated in Fig. 1. The data acquisition subsystem includes a belt scale, a tachometer wheel, a scanner, and a camera. The conveyor belt speed is measured by a tachometer. The conveyor belt scale and scanner measure the mass flow and volume flow of the muck on the conveyor belt, respectively. The camera fixed above the conveyor belt can continuously capture images of muck. The communication and control subsystems are used to transfer data and control the automatic starting and stopping of devices, including industrial network switches and power control modules. The data analysis subsystem is implemented on an industrial computer equipped with a graphics processing unit (GPU) for image analysis, data fusion, and data storage. The software subsystem integrates hardware, database, and data analysis into a web-based program, and realizes the visualization of information.

2.1. The data acquisition subsystem

The data acquisition subsystem is installed on the conveyer belt located in the TBM back-up system. Its structure is shown in Fig. 2, including a tachometer wheel, a belt scale, a scanner, and a camera. The transportation of muck uses an endless belt, including the upper and lower layer. The tachometer wheel and the belt scale are installed between the upper and lower layer of the belt. To prevent the sensors from being eroded and damaged in the harsh tunnel environment, the scanner and camera are packed in a steel box, which is fixed about 0.8 m above the belt and covered with a protective cover.

2.2. The communication and control subsystem

2.2.1. Data communication

The industrial computer located in the TBM control room is the core of the entire system. It is used for data processing, storage, and visualization. It is equipped with three independent network interface cards (NICs), which are connected to three different networks, as shown in Fig. 3. NIC 1 is connected with the data acquisition system for receiving data, including muck images, mass flow, volume flow data, and the parameters of the control module. In order to meet the needs of real-time image transmission, the data transmission rate of NIC 1 is 1Gbps. NIC 2 is connected to the TBM system. The real-time TBM operating parameters are obtained from the programmable logic controller (P.L.C.) of TBM at a frequency of 1 Hz and saved in the database of the computer. NIC 3 is connected to the Internet so that people outside the tunnel can view the current working status of the system through remote access. The data collected from different projects can also be uploaded to the cloud server to establish a comprehensive data warehouse.

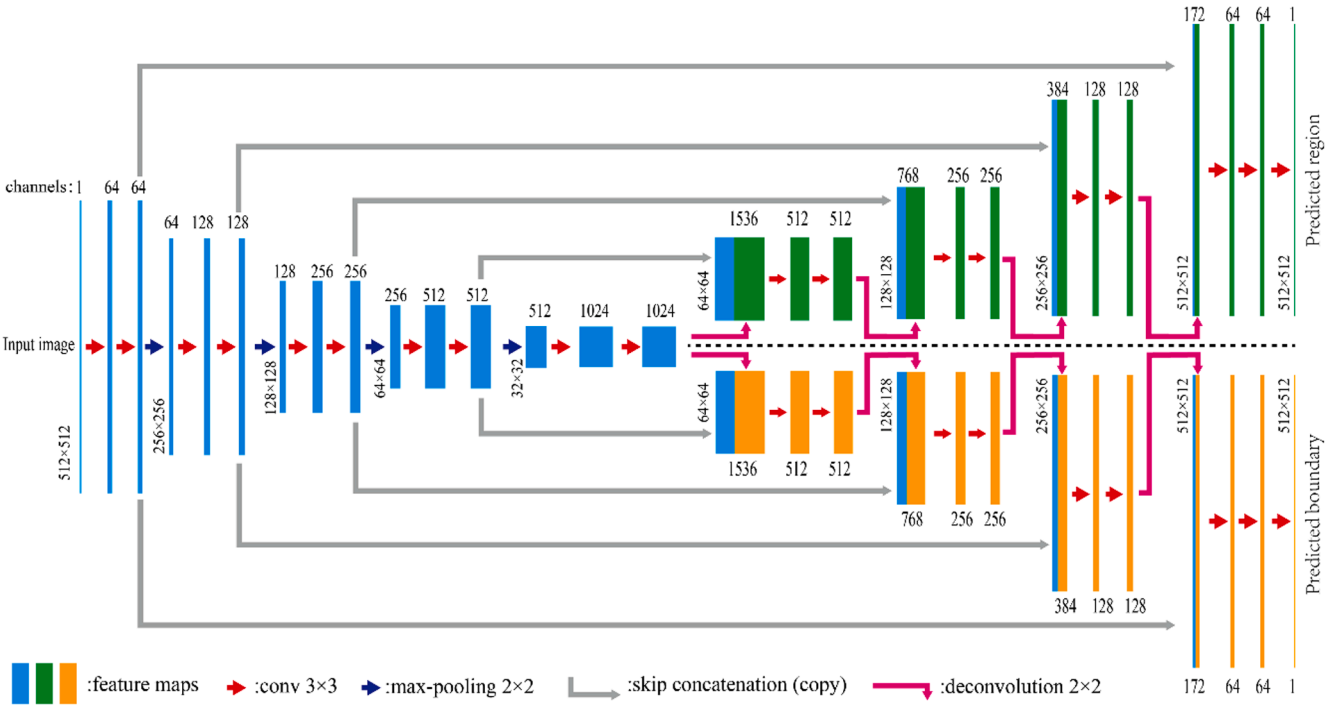

Fig. 5. The structure of the duple U-net model for image segmentation.

2.2.2. Automatic control

To synchronize the muck data acquisition with the TBM tunnelling, an automatic control system is designed and developed. The core component of the control system is a power control module, which can toggle the power status (active and inactive) of the scanner and camera. The control logic can be briefly described as follows. To continuously monitor the conveyor belt speed and the muck mass flow, the tachometer wheel, and the belt scale are always powered on, even in the TBM downtimes period. The conveyor belt speed and the mass flow are sent to the power control module in real-time to determine the mucking status. When the conveyor belt speed is higher than the speed threshold (0.5 m/s) and the mass flow is greater than the flow threshold (20 t/h), it means that there is muck transporting on the conveyor belt. Then, the power control module turn-on the power of the scanner and camera and make the system work normally. As the conveyor belt speed drops to 0 m/s, the power control module turns off the power and re-powers them again as the muck is detected. To continuously obtain TBM data and enable remote access, the industrial computer in the TBM control room is in a working state at all times.

2.3. The data analysis system

2.3.1. Database management

To store, retrieve, and manage different types of data, *MongDB*, which is an open-source document-oriented database and supports multiple data types, is used as a relational database management system (*RDBMS*). For this system, the *RDBMS* consisted of three primary data sources: engineering geological investigation data, TBM operating data, and muck data.

Engineering geological investigation data give a brief description of the geological condition along the tunnel alignment, e.g., lithologies, rock strength, faults, and groundwater conditions. This information can help the constructors to have a rough understanding of the rock mass conditions of the tunnel ahead. For the geological data of the excavated section, it can also be added to the database for further analysis.

TBM operating data is obtained through the communication interface of the PLC provided by the TBM equipment manufacturer. These data provide us with information about tunnelling mileage, TBM tunnelling posture, control parameters and performance parameters, etc., and are necessary for the interaction analysis between rock masses and TBM. Of which, the main parameters include thrust, torque, penetration, and RPM, etc.

The muck data includes the original data collected by the data acquisition system, as well as the rock chip characteristic data after image processing. Each group of images takes continuously 20–30 s. The particle size distribution of the muck is calculated for each group. Both mass and volume flow are recorded at 1 Hz and accumulated by time or mileage interval.

Besides, some parameters related to the system control, such as image acquisition duration, flow, and speed thresholds, are also stored in the database. These parameters can be modified according to the requirements of the project.

2.3.2. Image processing

The purpose of image processing is to extract valuable information about the interaction between rock masses and TBM from the muck images. This information can be represented by the features of the rock chips, including size, distribution, and shape, etc. To obtain these parameters, the most critical issue is to use image segmentation algorithms to detect the rock chips of images. However, the segmentation of muck images is extremely difficult for the following reasons. First, affected by the different rock mass conditions, the composition of the muck is very complicated. Usually, a muck image contains power, water, chips, and even mud in some particular cases. Thus, the algorithm has to be robust enough to handle various types of images. Secondly, rock chips vary widely in shape and size. The size distribution of rock chips generally ranges from 0.5 mm to 200 mm. This segmentation task with hugely different object sizes requires an algorithm that can extract both the local and global features of the image and make a reasonable pixel classification. Finally, the biggest challenge is to separate overlapping rock chips caused by stacking. The under-segmentation of overlapped rock chips contributes to the overestimate of the particle size.

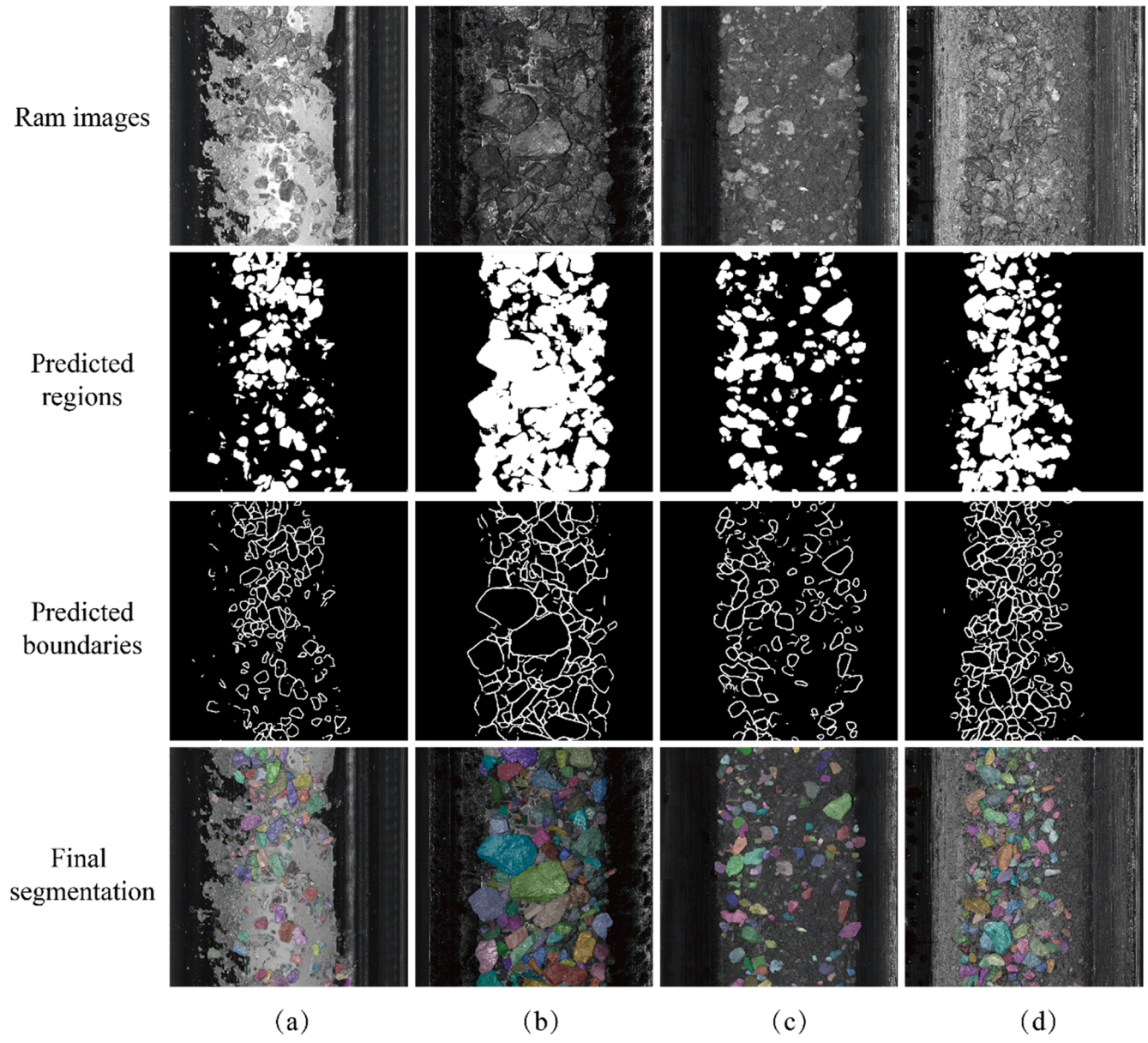

Fig. 6. Segmentation results of different types of muck images by duple U-net neural networks.

(1) Image segmentation

Benefited from the success of Convolutional Neural Networks(CNNs) in image segmentation and classification tasks, CNNs have become a powerful tool for solving the muck image segmentation. Among them, U-Net is one of the most promising deep learning frameworks for semantic image segmentation tasks. It is an end-to-end symmetric structure for pixel-wise segmentation, and includes two paths of down-sampling and up-sampling. It is proposed to solve the segmentation of neuron membrane images and achieves state-of-the-art performance. Since the aim of classic U-Net is to predict the class of pixel, it generally performs well in non-overlapping images. For images with severe overlap, the overlapped chips will be recognized as one. To separate overlapping rock chips, in the system, a duple U-Net network is proposed to predict the boundaries and regions of muck simultaneously, and combine morphological operations to achieve the final segmentation.

The overall process of image processing is presented in Fig. 4, including off-line stages and on-line stages. In the off-line stage, by using the collected muck images, the goal is to train a robust model for predicting regions and boundaries of chips. In the on-line stage, the trained model is used to deduce the regions and boundaries of the muck images captured in real-time, and the morphological operation is used to fuse the two parts to obtain the final segmentation result. Besides, after segmenting all the rock chips, the size features are extracted, and their size distribution is calculated.

In the off-line stage, some works were done to train the model,

Table 1
The extraction features of rock chips.

Feature	Description
long axis	length of minimum bounding rectangle
short axis	width of minimum bounding rectangle
major axis	major axis of equivalent ellipse
minor axis	minor axis of equivalent ellipse
area	area of chips
perimeter	perimeter of chips
ratio	the ratio of short axis to long axis

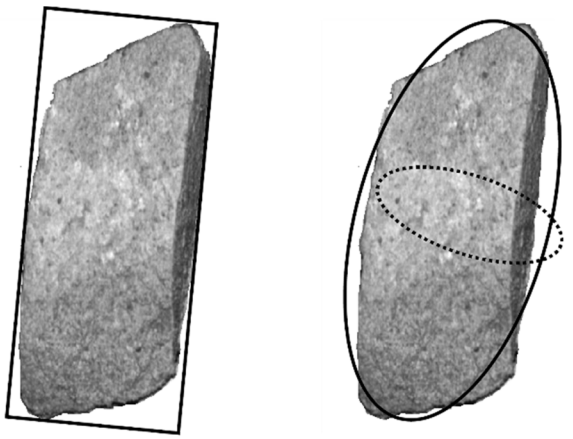

Fig. 7. Different size features of rock chips.

including image acquisition, chip labeling, and cropping, etc. Firstly, the system was installed in an in-situ TBM to track the tunnel excavation, and collected rich muck images under different rock mass conditions and boring parameters. After image acquisition, the representative images are selected to generate a dataset. To make sure that the trained model has better generalization ability, the chosen images should cover as many different geological conditions and boring parameters as possible, and allow at least 10 rock chips clearly-identifiable. Then, the clearly-identifiable rock chips in the chosen images, are manually labeled to create the ground truth data for evaluating predictions. The labeled images will be used to generate two kinds of binary mask, corresponding to the boundaries and regions of the rock chips, respectively. Before training, as the size of ram images is 2048 × 2048 pixels with a pixel size of 0.387 mm, all the full-size images and masks are cropped to 512 × 512 sub-images to meet the need of GPU memory. Then, the sub-images and their corresponding masks are fed to the duple U-net to conduct model training with the back-propagation algorithm. To refine the segmentation, both the boundaries and regions will be fused by morphological operations to get the final segmentation.

In the on-line stage, the real-time images are fed to the trained model to deduce the regions and boundaries of chips. Compared to the training process that requires a lot of time and resources, the real-time deduction can be much more efficient, during which a full-size image can be finished in 1–2 s using a single GPU. Owing to the full convolutional network (FCN) structure, the real-time full-size images can be directly fed to networks to obtain full-size regions and boundaries without cropping and merging under conditions of sufficient GPU memory. After that, the traditional morphology operators are applied to fuse the two masks. More specifically, the opening and closing operations are used to smooth the regions and eliminate noises, and the flood-fill algorithm is used to fill the holes in the regions. Last, to distinguish overlapped chips, the binary region mask is used to subtract the binary boundary mask. By detecting all the isolated regions, the main rock chips in the images can be are recognized.

The detailed structure of the dual U-Net network is shown in Fig. 5, which illustrates each operation from input to output. To take advantage of the similarity of the boundary and region in feature extraction, and improve the segmentation efficiency, the prediction of boundary and region are integrated into a unified network. It is an FCN that contains two branches of the encoder (down-sampling) and decoder (up-sampling). The role of the encoder is to extract the high-level features of the input image by multiple down-sampling blocks, whereas the decoder is to transform the high-level features into the full-resolution feature map for pixel-wise prediction. The encoder path includes four down-sampling blocks, with the ability to automatically extract the important features from images and integrate them into lower-resolution feature maps with multiple channels. Each block is embedded with

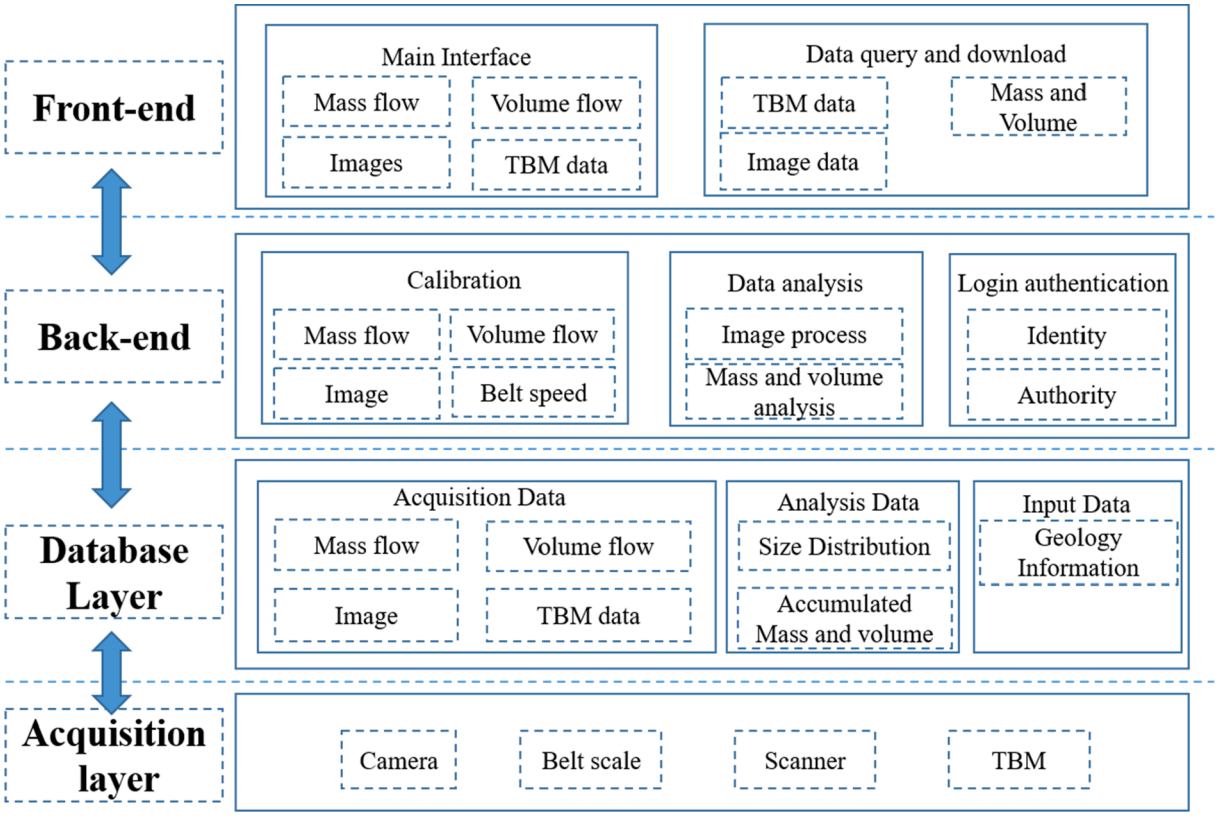

Fig. 8. The software architecture of the system.

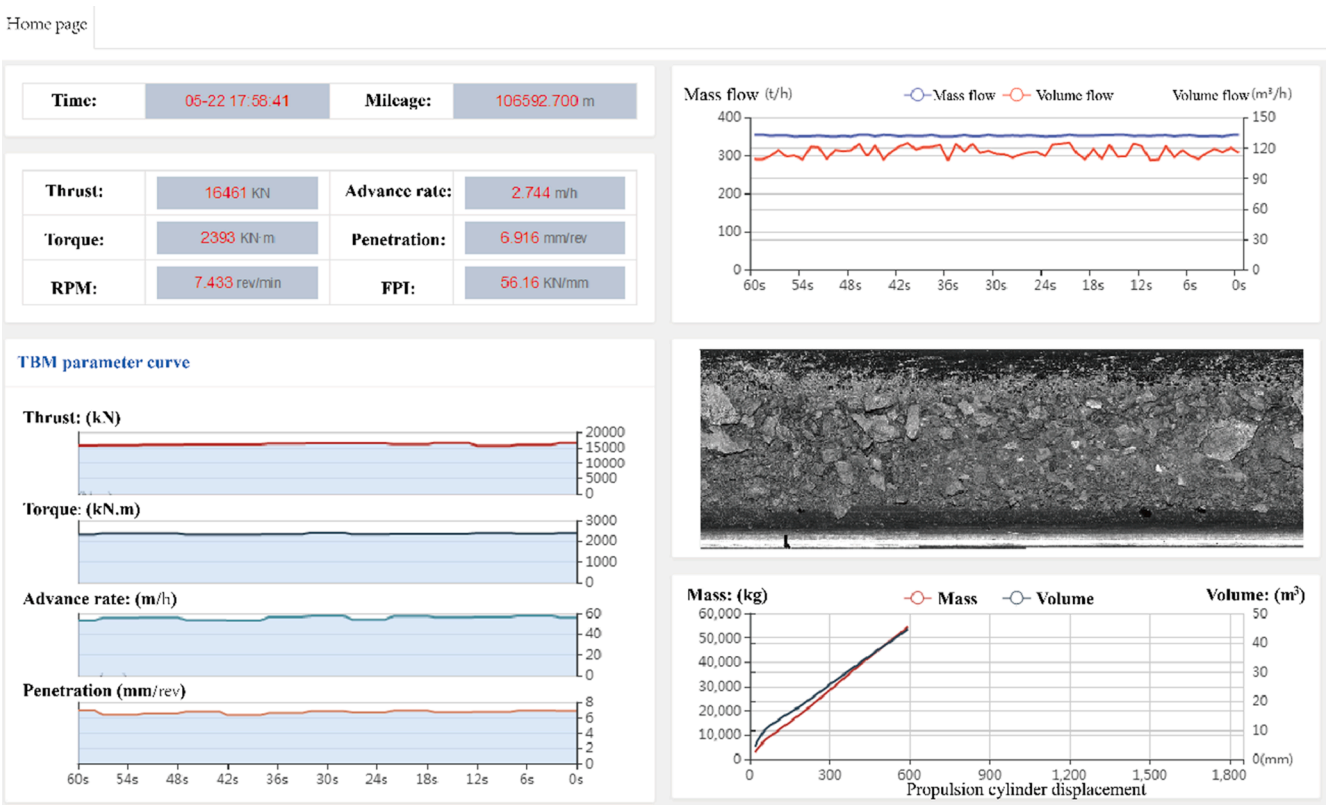

Fig. 9. The main interface of the system.

two convolutional layers activated by the Relu function (where $f(x) = \max(0,x)$) and a max-pooling layer with a size of 2 × 2. After each down-sampling block operation, the resolution of feature maps will be halved, and the number of channels will be doubled. Eventually, for an input image with 512 × 512 pixels, the encoder path will generate a feature map at a size of 32 × 32 with 1024 channels. For the decoder path, the predictions of boundary and region are two independent decoding processes with the same structure (it inherits the U-Net decoding part). For each decoder, it is symmetric to the encoder and also includes four up-sampling blocks. Compared with the down-sampling blocks, in the up-sampling blocks, the pooling layer is replaced by the deconvolution layer to restore the image resolution. In addition, the convolution operation also gradually reduces the number of channels of the feature maps to obtain the representation of the segmentation task. Correspondingly, after each up-sampling block operation, the resolution of feature maps will be doubled, while the number of channels will be halved. In the encoding process, the resolution of the feature maps is gradually reduced under the pooling operation, resulting in the loss of the spatial information, which is essential for finely pixels-wise prediction. To introduce the lost spatial information into the decoding process, for each up-sampling block, the feature map of the last layer of the previous up-sampling block is concatenated with the same-size intermediate map in the down-sampling block to form a combined map. Thus, the output feature map of each up-sampling block uses both the low-level features from the down-sampling and the high-level features from the up-sampling. This feature fusion runs through the entire decoding process, so that the U-Net structure obtains a more accurate segmentation compared with the basic FCN network. At the end of both decoders, the feature map is converted into a single-channel classification result through a convolution operation activated by the sigmoid function (where $f(x) = 1/(1 + e^{-x})$). The value represents the probability (between 0 and 1) that the pixel belongs to the foreground (region or boundary). By comparing with the probability threshold (set to 0.5), two masks representing the category of each pixel can be obtained.

During the training process, 100 images of 2048 × 2048 pixels are labeled and cropped into 1100 valid training images of 512 × 512 pixels. Each image has a corresponding ground truth annotation, describing the inner region and boundary of the rock chips. Some of them are used for training, and others are used as the test set to examine the performance of the model. In practice, network training is a process of optimizing parameters to minimize the difference between the outputs and the desired values. Based on the training data, the parameters of the network are iteratively adjusted with the back-propagation algorithm, and the network can automatically learn the mapping relationship between the image and the output masks. For an unseen image, the network can automatically deduce its region and boundary. It is worth noting that the network can only obtain the chip boundaries and regions of an input image, and the final segmentation results need to fuse these two parts.

Fig. 6(a)–(d) show the segmentation results of four typical muck images based on the proposed model. In the figure, (a) represents the muck containing a lot of muddy and water. Under the contrast of water, the rock chips can be easy to identify, and the segmentation result is satisfactory. As shown in Fig. 6(b), the muck mainly composed of large pieces of rock chips, which generally produced in the fractured rock mass. It is a big challenge to detect large and small objects at the same time, but the segmentation results show that the model has an excellent performance in handling this problem. Fig. 6(c)–(d) are the common types of muck under general rock mass conditions, corresponding to different boring parameters. For image (c), a large amount of rock powder produced during the rock breaking process covers many rock chips, so only the surface chips can be detected by the image analysis method. For particularly small chips, because its pixel volume is too few to provide enough information, the model recognizes it as a background. The image (d) contains a small amount of water and rock powder, and the rock chips are uniform in size. For this type of muck, accurate segmentation results can be achieved by our model. Because the model has different detection accuracy for small-sized chips in different kinds of

(a) the overall hardware diagram of the system (b) simulation experiment platform

Fig. 10. Indoor commissioning of the system.

muck, 10 mm is set as the minimum size threshold to ensure that the segmentation results are valid within the size range.

(2) Extraction of the rock chips feature and size distribution

Many studies have focused on the size and shape of the rock chips, which are most significantly affected by rock mass conditions and TBM operating parameters. The *OpenCV*, which is a computer vision library for image processing, is used to extract the contours and calculate the size features of the rock chips. The main features are shown in Table 1. The length and width of the minimum bounding rectangle, called as the short axis and long axis respectively, are used to represent the size of the rock chip, and the ratio of the short axis to the long axis is to describe the shape of the rock chip, as shown in Fig. 7(a). To obtain the volume-based size distribution, each particle is assumed to be an ellipsoid and mapped from 2D to 3D, as shown in Fig. 7(b). The volume can be calculated as $4\pi(ab^2)/3$, where a and b are the major and minor axis of the equivalent ellipse, respectively. Moreover, the area and the perimeter are also calculated. In the system, the particle size distribution is characterized by the short axis. For the intact rock mass, the short axis of most rock chips will not exceed the disc cutter spacing, but it has a more widely distributed for jointed rock masses. Thus, using the short axis as the characteristic size can support to distinguish the rock mass conditions.

2.4. The software system

To manage the real-time analysis of high volume streaming data, an efficient software needs to be developed. Moreover, the software also has to provide users with functions like information visualization, data query, user management, etc. Considering these requirements, software architecture is shown in Fig. 8. The front-end and back-end of the software are developed using JavaScript and Java, respectively. Image analysis is the most time-consuming part of the software system. To improve efficiency, the image analysis algorithm is written in *C++* programming language that has better efficiency than Java, based on the deep learning frameworks *Tensorflow* 1.13, and built as a *Dynamic Link Library* (DLL) for back-end programs to call. The system interface is web-based so that users can use a browser to access the system from any connected devices without installing any software or tools. To provide real-time visual information, the user interface should be convenient and easy-to-use for the operators.

Fig. 9 shows the screenshot of the main interface of the system. It mainly displays real-time monitoring information from three aspects: TBM operating parameters, mass and volume flow and muck images. The real-time values and time curve of the vital TBM parameters, e.g., thrust, torque and penetration, are shown in the left of the figure, and are used to help the operator observe the changing trend of these parameters. In the upper right corner of the figure, the mass and volume flow curves within one minute (the user can reset it according to the situation) are shown in blue and red, respectively, to monitor the mucking status of TBM tunnelling. When the tunnel face collapses, the mass and volume curve will be much higher than the normal level. However, due to tunnelling, the flow curves are not stable but have significant vibration, so the stability of the tunnel face cannot be

Table 2
Verification of measurement errors of the accumulated mass and volume.

No	Actual weight (kg)	Actual volume (m^3)	Measured weight (kg)	Measured volume (m^3)	Weight error (%)	Volume error (%)
1	296.4	0.1766	294.1	0.1834	−0.78%	3.83%
2	288.1	0.1716	284.3	0.1655	−1.32%	−3.55%
3	294.4	0.1755	297.6	0.1776	1.09%	1.20%
4	283	0.1685	288.2	0.1737	1.84%	3.09%
5	310.2	0.1849	309.05	0.1825	−0.37%	−1.28%

Fig. 11. The open-type TBM used in tunnel construction.

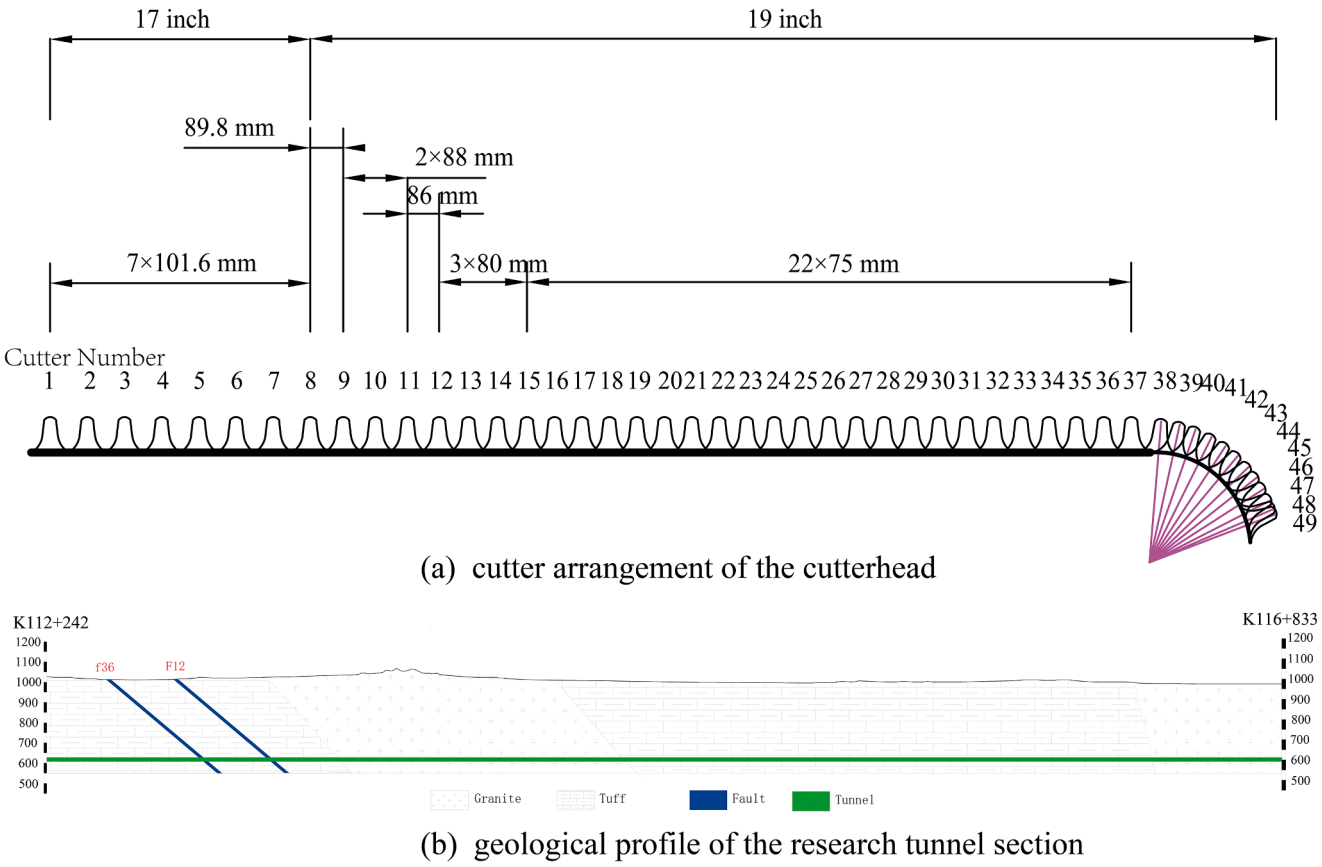

Fig. 12. The cutter arrangement of the cutterhead and geological profile of the research tunnel section.

Table 3
Technical characteristics of TBM.

Technical parameter	Design value
Cutterhead diameter (mm)	7030
Maximum cutterhead power (kW)	8 × 350 = 2800
Minimum horizontal turning radius (m)	500
Thrust (kN)	19635@250 bar 27488kN@350 bar
Cutterhead torque (kN.m)	5664 (@4.72 rpm) 2970 (@9.0 rpm)
Numbers of disc cutters	49
Total TBM weight (tons)	Approx.1400

determined based on short-term data. To further visualize the change in muck amount, for each stroke, the curves of the accumulated mass and accumulated volume verse the displacement of the propulsion cylinder are shown in the lower right corner of the figure. For an intact rock mass, assuming a small change in the rock mass density, the stepwise cumulative curve should be an inclined straight line. If the monitored curve has a "hump", it may indicate that the tunnel face has collapsed. In the middle right of the figure, the real-time muck images are played in turn. Although these images will be processed into quantitative size distribution information, some morphological features, e.g., water and mud, can help operators to judge rock mass conditions more accurately.

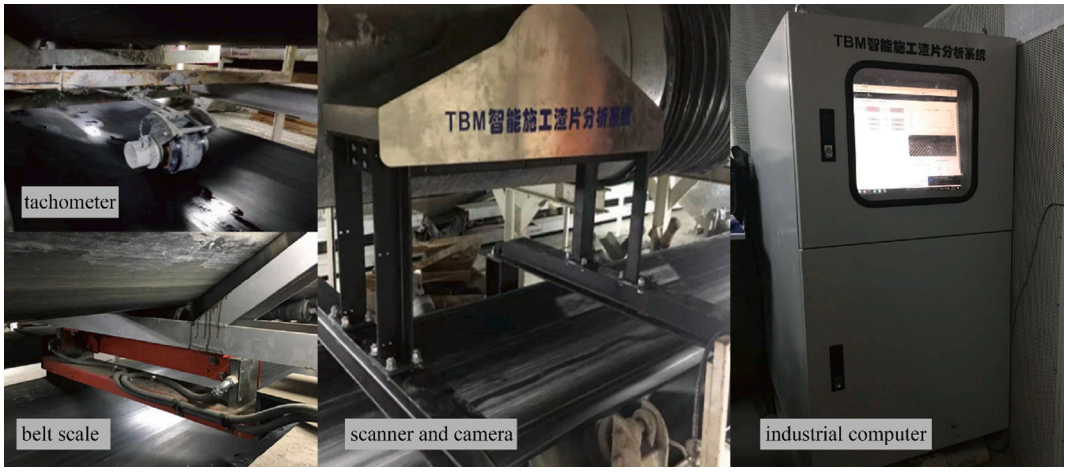

Fig. 13. The system installed in site.

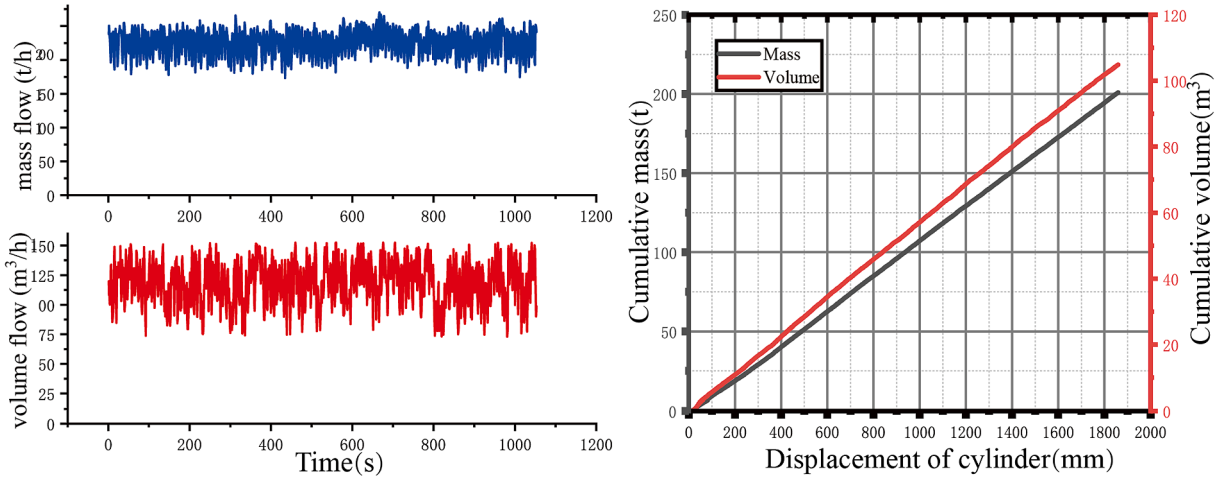

(a) The real-time monitored mass flow and volume flow (b) cumulative mass and volume of muck vs the cylinder's displacement

Fig. 14. The monitoring results of mass and volume.

3. System commissioning

In purpose to verify the system design and the accuracy of measurements, an indoor experimental platform was established to simulate the mucking process of TBM tunnelling, as shown in Fig. 10. The rock chips were replaced by rock debris with an average diameter of 1 cm. This material has a relatively uniform size and shape, so the loose volume can be accurately estimated by dividing its mass by loose density. With multiple measurements, the loose density of the debris is 1678 kg/m^3. After that, the belt scale was calibrated following the manufacturer recommendations before testing. In the simulated environment, the measurement errors of the mass flow and volume flow of the system were verified, and the imaging effect of the camera was also tested. The total mass of the debris used in each test was about 300 kg, and the five test results are given in Table 2. The test results show that the mass and volume measurement errors of the system are within ±2% and ±4%, respectively.

4. Engineering application of the system

4.1. Project overview

This system is installed and applied to a TBM tunnelling project in China. The total length of the tunnel section is about 29.027 km, and the designed longitudinal slope is less 1/2000. Among them, the length of the TBM excavation section is 23.624 km, and is constructed by a full-face hard rock TBM manufactured by China Railway Engineering Equipment Group Co., Ltd, as shown in Fig. 11. The cutterhead has a diameter of 7.03 m, and is equipped with 49 disc cutters, including 8 17-in. central cutters, 29 19-in. normal cutters, and 12 19-in. side cutters. The cutter arrangement of the cutterhead is as shown in Fig. 12(a). The design specifications of the TBM are shown in Table 3.

The geological profile of the research section is shown in Fig. 12(b). It is worth explaining that the information presented was obtained from the geological investigation stage. Still, the actual rock mass conditions revealed after the excavation may differ from those in the geological investigation stage.

4.2. In site installation

The mucking system of the TBM consists of three section conveyor belts, namely the host conveyor belt, the back-up conveyor belt, and the continuous conveyor belt. The host conveyor belt comes out from the cutterhead, and extends to the end of the main beam, and transports the muck to the back-up conveyor belt. Then, the back-up conveyor belt carries the muck to the end of TBM and drops it to the continuous conveyor belt, which is long and extends to the outside the tunnel. Because the length of the host conveyor belt is short, the impact force of the muck falling from the mucking hole may cause a significant change in the tension of the belt, which will affect the accuracy of weighing. Besides, the host conveyor belt is located under the working platform, so there is not enough space to install the acquisition system. Although the continuous conveyor belt avoids the above mentioned disadvantages of the host belt, the installed system cannot follow the movement of the TBM, resulting in longer and longer monitoring information delays. The back-up conveyor belt has enough installation space and a relatively stable belt tension force, so it is the most suitable one for installing the acquisition devices. Fig. 13 presents photos of the subsystem installed in-site. The installation position is about 150 m from the tunnel face. As the muck is transferred from tunnel face to the acquisition system, there is an information delay of about 40 s. During this period, the geological conditions can be considered no change so that the delay can be ignored. The industrial computer is located in the TBM control room, allowing the operator to obtain the feedback from the system directly.

4.3. Monitoring of muck mass flow and volume flow

Fig. 14(a) shows the curves of the muck mass and volume flow monitored by the system in the stable tunnelling state. It can be seen from the figure that both the mass and volume flow curves have apparent oscillations, indicating that the muck amount on the belt is continuously changing. Compared with the mass flow, the amplitudes of change in volume flow are larger. The possible reason is that the volume flow is affected by the random accumulation of rock chips on the belt. Fig. 14(b) shows the cumulative mass and volume changed with the displacement of the propulsion cylinder. Although the flow curve is oscillating, the changes in cumulative mass and volume are linear with the displacement of the propulsion cylinder. It means that no collapse of the tunnel face occurs during this stroke, which is consistent with the actual surrounding rock mass conditions observed after the excavation.

The displacement increment of the propulsion cylinder during the excavation is 1800 mm, and it can also be considered as the excavation length. The cumulative mass and volume monitored by the system are 200.93 t and 104.85 m^3, respectively. As the rock mass is stable, according to the tunnel diameter and excavation length, the theoretical excavation volume is calculated to be 69.85 m^3. Further, the density of

Fig. 15. Tunnel wall photographs and muck images for two rock mass conditions.

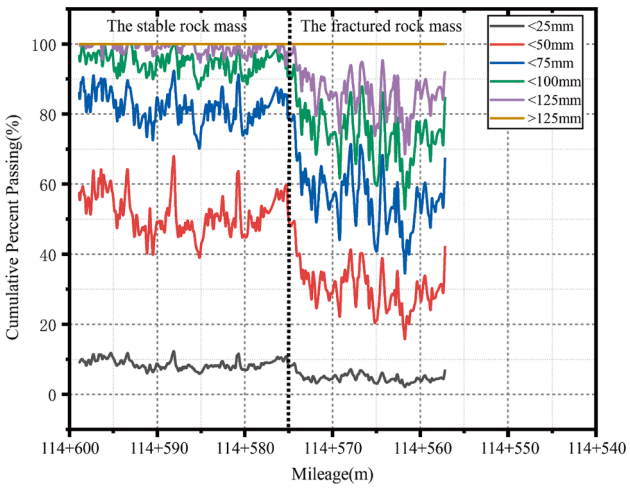

Fig 16. The distribution of chips obtained by image analysis.

the rock mass can be estimated to be about 2870 kg/m^3, and the loose coefficient of the muck is about 1.50. Compared with the actual rock mass density (2700 kg/m^3), the measured rock mass density of the system is slightly larger, which may be attributed to two reasons. On the one hand, due to the long-term operation and daily maintenance, e.g., belt vulcanizing and belt correction, the belt tension has changed. Hence, the belt scale and scanner should be recalibrated frequently in daily use. On the other hand, during the tunnelling process, the cutter head continuously jets water to lower the temperature of the cutter and remove dust. The weight of this water is also accumulated into the mass of the muck. Combining these two factors, the measured value of the muck mass will deviate from the actual value.

Apart from these above mentioned factors during construction, there are still many uncertain parameters in calculating the theoretical mass and volume (without overbreak), e.g., the rock mass density and the loose coefficient(Mooney et al., 2012). Due to the lack of reference, the monitored mass and volume values cannot be directly used to judge the overbreak of the tunnel. However, this does not mean that mass and volume monitoring is meaningless. Actually, in a small section of the rock mass, these uncertain parameters change so little that they can be

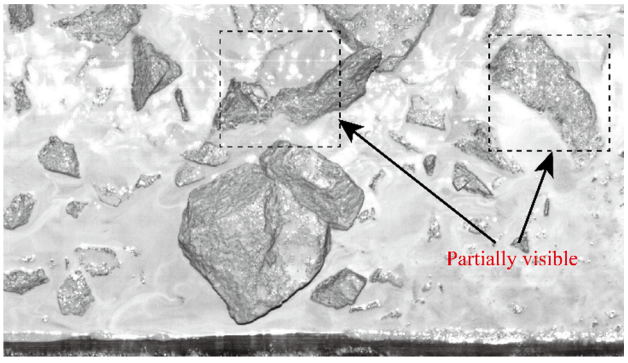

(a) muck with mud and water

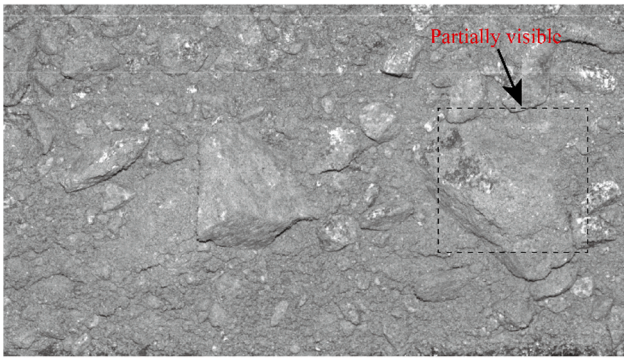

(b) muck with a lot of fines

Fig. 17. Examples of muck images with mud or a lot of fines.

considered as a constant. To estimate them, the back-analysis method can be used for the excavated data. Specifically, after excavation, the overbreak state of the surrounding rock mass can be determined by observation in the support area. Thus, according to the monitored mass and volume of the muck and the actual excavation volume of the rock mass, their rock mass density and loosening coefficient can be calculated. For the unexcavated rock mass, the theoretical mass and theoretical volume can be estimated from the parameters of the adjacent excavated section. Because it needs to tolerate a narrow range of parameters changes, this method may not be used to monitor small overbreak. However, for TBM construction, the large collapses in the tunnel face and surrounding rock masses are the primary concern of TBM tunnel construction. Apart from this, the changes in mass flow and volume flow can also help to estimate the rock mass stability. During the tunnelling process, as the tunnel face collapses, the instantaneous flow of muck and volume will increase significantly. These specific relationships need to be explored further from more engineering data.

4.4. Image analysis of muck

Image analysis of muck is carried out in a section of granite formation about 45 m in length, with the chainage ranged from 114 + 600 to 114 + 555. After excavation, the tunnel wall reveals that there are two classes of rock mass in this section. In the section of 114 + 600 ~ 575, the rock mass is composed of slightly weathered granite. A main joint set is found in the rock mass. The joint spacing is about 200–400 mm. The surrounding rock mass has good stability, as shown in Fig. 15 a (i). In the section of 114 + 575 ~ 555, the rock mass is pervasively jointed and weathered. Three sets of joints are observed, and the joint spacings are 50–100 mm, 100–200 mm, 200–400 mm respectively. Some joints are filled with clay minerals or marked with iron staining. Some collapse cavities can be found at the top and left of the tunnel wall, as shown in Fig. 15 a (ii).

The particle size distribution obtained by image analysis is shown in Fig. 16. At chainage 114 + 575, the size distribution has changed significantly, which is consistent with the change of the rock mass class. For the relatively intact rock mass, the cumulative percent passing at the same sieve size is much higher than that of the fractured rock mass, indicating that the overall size is smaller, as shown in Fig. 15 b (ii) . Because there are fewer joints in the rock mass, the rock chips are mainly formed by the lateral cracks produced by the adjacent disc cutters. Hence, the size of the chip is small, and a lot of rock powder is generated with the rock breaking. However, as it is tough to segment small chips, the proportion of debris (<10 mm) is not reflected in the image processing results. For the fractured rock mass, the overall particle size is larger. One of the significant differences is that the proportion of >125 mm is about 16%, but it is 0 for the relatively intact rock mass. It indicates that the muck contains many large block chips, which can be seen from the image in Fig. 15 b (ii). For the jointed rock masses, the joint planes divide the rock mass into blocks. The crack caused by the cutter penetration propagates to the joint planes and forms the chips. Therefore, these chips are mainly block-shaped with large size.

On the base of the above analysis, it is concluded that the image analysis results obtained by the system can directly reflect the changes in the rock mass conditions. Hence, it can provide valuable information for assisting TBM tunnelling. However, this paper only qualitatively analyzed the correlation between the particle size distribution of the muck and the rock mass to verify the application value of the system. To realize the rock mass prediction ahead of the tunnel face and assist TBM optimum tunnelling, more engineering rock mass data and the corresponding muck data are needed. Besides, since the TBM operating parameters also affect the shape and size of the muck, the correlation also needs to be considered in future studies.

4.5. Limitations

Despite the developed system demonstrating satisfactory performance in muck analysis, it still has some limitations in some situations, especially for the muck with mud or a large amount of powder. For these types of muck, due to the surface covered with fines, water or mud, most chips are not available to be captured completely by the image acquisition system as shown in Fig. 17. As a result, the image segmentation performs poorly for evaluating the size distribution of rock chips as it can only detect part of a chip. Hence, the current image segmentation strategy cannot handle these problems well. However, these types of muck should be paid more attention due to their relations with faults or highly weathered rock masses. Fortunately, these types of muck have distinctive image characteristics, such as high brightness, gloss, or powdery texture. Some new methods can be introduced to distinguish them from others, such as pattern recognition or image classification. These technologies focus on the overall analysis of images rather than the pixel-level features and show better robustness in processing the overall analysis of images. This work requires a dataset of various types of images, and will be carried out in future.

5. Conclusion

The muck provides rich information for the rock mass prediction ahead of the tunnel face and evaluation of the rock-breaking efficiency. A muck analysis system for assistant intelligence TBM tunnelling has been proposed and developed. The system consists of a data acquisition system, communication and control system, data analysis system and software system. It can simultaneously collect the real-time image, mass flow and volume flow of the muck. The system applied the image processing algorithm with a dual U-net network structure based on deep learning to efficiently process image segmentation and feature extraction. The measurement accuracy is verified by a series of experiments in the simulation test platform. Then, it is applied to a practical TBM tunnelling project. The application results indicate that the size distribution of the muck, obtained by the image analysis in the system, can well reflect the changes of the rock mass conditions. The monitored mass

and volume of the muck also are in accord with the theoretical calculations. The system achieved its design requirements and functions, and can provide muck analysis data for further assistant intelligent TBM tunnelling.

CRediT authorship contribution statement

Qiuming Gong: Conceptualization, Methodology, Supervision. **Xiaoxiong Zhou:** Data curation, Writing - original draft, Software, Visualization. **Yongqiang Liu:** Investigation. **Bei Han:** Validation. **Lijun Yin:** Writing - review & editing.

Declaration of Competing Interest

The authors declare that they have no known competing financial interests or personal relationships that could have appeared to influence the work reported in this paper.

Acknowledgments

We are grateful to Beijing Jiurui Technology Co., Ltd for their technical support in system development. We also would like to thank China Railway Tunnel Stock Co., Ltd, and China Railway Construction Heavy Industry Co. Ltd and China Railway Engineering Equipment Group Co., Ltd. for their cooperation in the in-situ application of the system.

References

Abu Bakar, M.Z., Gertsch, L.S., Rostami, J., 2014. Evaluation of fragments from disc cutting of dry and saturated sandstone. Rock. Mech. Rock. Eng. 47 (5), 1891–1903.
Barton, N.R., 2000. TBM Tunnelling in Jointed and Faulted Rock. Crc Press.
Bruland, A., 2000. Hard rock tunnel boring. Fakultet for ingeniørvitenskap og teknologi.
Entacher, M., Galler, R., 2013. Development of a disc cutter force and face monitoring system for mechanized tunnelling / Ortsbrustmonitoring und Leistungsprognose bei TBM-Vortrieben. Geomechanik Tunnelbau 6 (6), 725–731.
Entacher, M., Winter, G., Bumberger, T., Decker, K., Godor, I., Galler, R., 2012. Cutter force measurement on tunnel boring machines – System design. Tunn. Undergr. Space Technol. 31, 97–106.
Entacher, M., Winter, G., Galler, R., 2013. Cutter force measurement on tunnel boring machines – Implementation at Koralm tunnel. Tunn. Undergr. Space Technol. 38, 487–496.
Erben, H., 2016. Real-Time Material Analysis and Development of a Collaboration and Trading Platform for Mineral Resources from Underground Construction Projects.
Farrokh, E., Rostami, J., 2008. Correlation of tunnel convergence with TBM operational parameters and chip size in the Ghomroud tunnel, Iran. Tunn. Undergr. Space Technol. 23 (6), 700–710.
Gao, X., Shi, M., Song, X., Zhang, C., Zhang, H., 2019. Recurrent neural networks for real-time prediction of TBM operating parameters. Autom. Constr. 98, 225–235.
Gong, Q., She, Q., Wang, J., Hou, Z., Wu, S., 2010. Influence of different thicknesses of marble layers on TBM excavation. Chinese J. Rock Mech. Eng. 7, 1442–1449 (in Chinese).
Gong, Q.M., Jiao, Y.Y., Zhao, J., 2006. Numerical modelling of the effects of joint spacing on rock fragmentation by TBM cutters. Tunn. Undergr. Space Technol. 21 (1), 46–55.
Gong, Q.M., Zhao, J., 2009. Development of a rock mass characteristics model for TBM penetration rate prediction. Int. J. Rock Mech. Min. Sci. 46 (1), 8–18.
Gong, Q.M., Zhao, J., Jiang, Y.S., 2007. In situ TBM penetration tests and rock mass boreability analysis in hard rock tunnels. Tunn. Undergr. Space Technol. 22 (3), 303–316.
Gong, Q.-M., Zhao, J., Jiao, Y.-Y., 2005. Numerical modeling of the effects of joint orientation on rock fragmentation by TBM cutters. Tunn. Undergr. Space Technol. 20 (2), 183–191.
Hamidi, J.K., Shahriar, K., Rezai, B., Rostami, J., 2010. Performance prediction of hard rock TBM using Rock Mass Rating (RMR) system. Tunn. Undergr. Space Technol. 25 (4), 333–345.
Heydari, S., Khademi Hamidi, J., Monjezi, M., Eftekhari, A., 2019. An investigation of the relationship between muck geometry, TBM performance, and operational parameters: a case study in Golab II water transfer tunnel. Tunn. Undergr. Space Technol. 88, 73–86.
Huang, X., Liu, Q., Liu, H.e., Zhang, P., Pan, S., Zhang, X., Fang, J., 2018. Development and in-situ application of a real-time monitoring system for the interaction between TBM and surrounding rock. Tunn. Undergr. Space Technol. 81, 187–208.
Jiang, M., Liao, Y., Wang, H., Sun, Y.a., 2018. Distinct element method analysis of jointed rock fragmentation induced by TBM cutting. Eur. J. Environ. Civil Eng. 22 (sup1), s79–s98.
Li, S., Liu, B., Xu, X., Nie, L., Liu, Z., Song, J., Sun, H., Chen, L., Fan, K., 2017. An overview of ahead geological prospecting in tunneling. Tunn. Undergr. Space Technol. 63, 69–94.
Li, S., Nie, L., Liu, B., 2018. The practice of forward prospecting of adverse geology applied to hard rock TBM tunnel construction: the case of the songhua river water conveyance project in the middle of Jilin province. Engineering 4 (1), 131–137.
Liu, J., Cao, P., Han, D., 2016. The influence of confining stress on optimum spacing of TBM cutters for cutting granite. Int. J. Rock Mech. Min. Sci. 88, 165–174.
Liu, Q., Liu, J., Pan, Y., Kong, X., Hong, K., 2017. A case study of TBM performance prediction using a Chinese rock mass classification system – Hydropower Classification (HC) method. Tunn. Undergr. Space Technol. 65, 140–154.
Liu, X., Xu, M., Qin, P., 2019. Joints and confining stress influencing on rock fragmentation with double disc cutters in the mixed ground. Tunn. Undergr. Space Technol. 83, 461–474.
Maleki, M.R., 2018. Rock Joint Rate (RJR); a new method for performance prediction of tunnel boring machines (TBMs) in hard rocks. Tunn. Undergr. Space Technol. 73, 261–286.
Mohammadi, M., Khademi Hamidi, J., Rostami, J., Goshtasbi, K., 2020. A closer look into chip shape/size and efficiency of rock cutting with a simple chisel pick: a laboratory scale investigation. Rock Mech. Rock Eng. 53 (3), 1375–1392.
Mooney, M.A., Walter, B., Frenzel, C., 2012. Real-time tunnel boring machine monitoring: A state-of-the-art review. In: 2012 Proceedings - North American Tunneling, NAT 2012, pp. 73–81.
Naghadehi, M.Z., Samaei, M., Ranjbarnia, M., Nourani, V., 2018. State-of-the-art predictive modeling of TBM performance in changing geological conditions through gene expression programming (vol 126, pg 46, 2018). Measurement 130, 482–482.
Oggeri, C., 2017. Tunnelling muck classification: definition and application. In: Proceedings of the World Tunnel Congress, Bergen, Norway.
Rispoli, A., Ferrero, A.M., Cardu, M., Farinetti, A., 2017. Determining the particle size of debris from a tunnel boring machine through photographic analysis and comparison between excavation performance and rock mass properties. Rock Mech. Rock Eng. 50 (10), 2805–2816.
Rostami, J., 1997. Development of a force estimation model for rock fragmentation with disc cutters through theoretical modeling and physical measurement of crushed zone pressure. Colorado School of Mines Golden.
Salimi, A., Faradonbeh, R.S., Monjezi, M., Moormann, C., 2018. TBM performance estimation using a classification and regression tree (CART) technique. Bull. Eng. Geol. Environ. 77 (1), 429–440.
Slinchenko, D., 2009. Control of ground settlement in EPB Tunneling. In: Proceedings of the ITA-IATES World Tunnel Congress.
Sun, W., Shi, M., Zhang, C., Zhao, J., Song, X., 2018. Dynamic load prediction of tunnel boring machine (TBM) based on heterogeneous in-situ data. Autom. Constr. 92, 23–34.
Tuncdemir, H., Bilgin, N., Copur, H., Balci, C., 2008. Control of rock cutting efficiency by muck size. Int. J. Rock Mech. Min. Sci. 45 (2), 278–288.
Vergara, I.M., Saroglou, C., 2017. Prediction of TBM performance in mixed-face ground conditions. Tunn. Undergr. Space Technol. 69, 116–124.
Yin, L., Miao, C., He, G., Dai, F., Gong, Q., 2016. Study on the influence of joint spacing on rock fragmentation under TBM cutter by linear cutting test. Tunn. Undergr. Space Technol. 57, 137–144.
Yin, L.J., Gong, Q.M., Zhao, J., 2014. Study on rock mass boreability by TBM penetration test under different in situ stress conditions. Tunn. Undergr. Space Technol. 43, 413–425.
Zhai, S.F., Zhou, X.P., Bi, J., Xiao, N., 2016. The effects of joints on rock fragmentation by TBM cutters using General Particle Dynamics. Tunn. Undergr. Space Technol. 57, 162–172.
Zhang, Q., Liu, Z., Tan, J., 2019. Prediction of geological conditions for a tunnel boring machine using big operational data. Autom. Constr. 100, 73–83.
Zhao, J., Shi, M., Hu, G., Song, X., Zhang, C., Tao, D., Wu, W., 2019. A data-driven framework for tunnel geological-type prediction based on TBM operating data. IEEE Access 7, 66703–66713.